

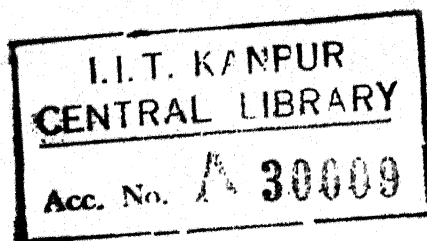
FABRICATION, ANALYSIS AND EXPERIMENTAL STUDY OF A CYLINDRICAL SOLAR WATER HEATER

**A Thesis Submitted
In Partial Fulfilment of the Requirements
for the Degree of
MASTER OF TECHNOLOGY**

**By
ANIL KUMAR RAJVANSHI**

to the

**DEPARTMENT OF MECHANICAL ENGINEERING
INDIAN INSTITUTE OF TECHNOLOGY KANPUR
AUGUST 1974**

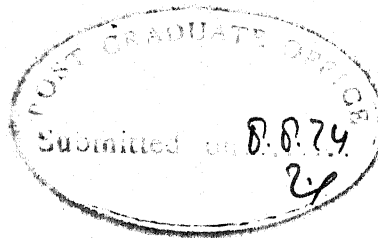


27 AUG 1974



ME-1974-M-RAJ-FAB

Shesir
621.47
R13



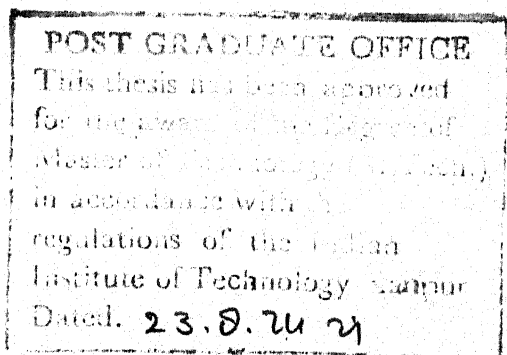
ii

CERTIFICATE

This is to certify that the work on "Fabrication, Analysis and Experimental Study of a Cylindrical Solar Water Heater" has been carried out under my supervision and has not been submitted elsewhere for a degree.

V. Kadambi

V. KADAMBI
Professor and Head
Department of Mechanical Engineering
Indian Institute of Technology, Kanpur



ACKNOWLEDGEMENT

The author wishes to express his gratitude and indebtedness to Professor V. Kadambi for his valuable guidance and constant encouragement throughout the course of this investigation.

The author is grateful to Mr. N. Ravichandran, Mr. S.K. Chaturvedi and Mr. Mithileshwar Prasad for their useful suggestions during the course of study.

Sincere thanks are also due to Mr. S. Verma of Civil Engineering Department for supplying the graphs of Solar radiation measurements. The work of Mr. P.N. Mishra and Mr. Mushtaq Ali in helping to set up the experimental apparatus is also appreciated.

Finally, but not the least, the author wishes to thank Mr. J.D. Varma for his excellent typing of the manuscript.

Anil Kumar Rajvanshi

CONTENTS

	Page
LIST OF TABLES	v
LIST OF FIGURES	vi
NOMENCLATURE	vii
ABSTRACT	ix
CHAPTER I : INTRODUCTION	1
1.1 : Need for Solar Energy Utilization	1
1.2 : Availability of Solar Energy	2
1.3 : Harnessing of Solar Energy	3
1.4 : Review of Previous Work	4
1.5 : Motivation for the Present Work	7
CHAPTER II : THEORETICAL ANALYSIS	10
2.1 : Energy Balance Equations	13
2.2 : Evaluation of Constants and Heat Flux q	17
2.3 : Method of Solution	21
CHAPTER III : EXPERIMENTAL SET UP	24
3.1 : Apparatus	24
3.2 : Instrumentation	28
3.3 : Modes of Test	29
CHAPTER IV : RESULTS AND DISCUSSIONS	31
4.1 : Results	31
4.2 : Conclusions and Recommendations	43
REFERENCES	45
APPENDIX I : Computer Programme	47

LIST OF TABLES

		Page
Table 2-1	Transmittivities, Absorptivities and Emissivities of glass and metal surface	21
Table 4-1	Experimental data and results for test in natural convection (May 18, 1974)	31
Table 4-2	Experimental data and results for tests in continuous flow.	34
Table 4-3	Comparison of experimental and theoretical results of heater under forced convection mode.	42

LIST OF FIGURES

	Page
Figure 1-1	Tube type solar water heater 5
Figure 1-2	Corrugated sheet type solar water heater 5
Figure 2-1	Sectional view of the experimental apparatus 11
Figure 3-1	Line diagram of the experimental set up 26
Figure 3-2	Positions of the thermocouples on the metallic tube 28
Figure 4-1	Experimental results for test in natural convection (May 18, 1974) 32
Figure 4-2	Experimental results for test in forced convection (May 29, 1974) 34
Figure 4-3	Experimental results for test in forced convection (May 31, 1974) 36
Figure 4-4	Experimental results for test in forced convection (June 2, 1974) 37
Figure 4-5	Experimental results for test in forced convection (June 12, 1974) 38
Figure 4-6	Comparison of the experimental and theoretical results. 31

NOMENCLATURE

A_n	Constant in Eq. (4)
C_2	Functions defined in Eq. (9) and Eq. (10)
c_p	Specific heat of the liquid, kcal/kg - °C
D	Diameter, m
F_D	Shape factor between the ground and the heater
F_{i-j}	View factor for radiant exchange between surfaces, i and j, of two coaxial cylinders
$g(x^*)$	A function specified in Eq. (4)
H	Hour angle, radians
h_a	Heat transfer coefficient between outer glass surface and air, kcal/m ² - h - °C
k	Thermal conductivity, kcal/m - h - °C
\dot{m}	Mass-flow rate of liquid through the tube, kg/h
Pr	Prandtl number for liquid, $\mu c_p / k_f$
q	Average incident radiation intensity over the outer glass tube, kcal/m ² -h
$q_o(x^*)$	Effective average energy flux over the metal tube surface, kcal/m ² - h
r	Reflectivity
Re	Reynold's number based on tube diameter and liquid kinematic viscosity
R_{Df}	Diffuse sky radiation, kcal/m ² -h
R_{DN}	Direct normal radiation, kcal/m ² -h
R_{GR}	Ground reflected radiation, kcal/m ² -h

r_g	Ground reflectance
R_s	Orientation factor for sky radiation
T	Absolute temperature, $^{\circ}\text{K}$
T_a	Outside air temperature, $^{\circ}\text{C}$
T_e, T_m	Entering fluid and mixed mean temperatures respectively, $^{\circ}\text{C}$
U_{i-j}	Overall heat transfer coefficient between surfaces i and j $\text{kcal/m}^2 - \text{h} - ^{\circ}\text{C}$
x	Axial coordinate, measured from inlet, m
x^*	Non dimensionalised axial coordinate specified by Eq. (6)
α	Absorptivity to radiation
β	Altitude angle, degrees
ϵ	Surface emissivity
η	Collector efficiency for tube length x
λ_n	The n^{th} eigenvalue in Eq. (4)
ϕ	Solar azimuth angle, degrees
ψ	Angle of inclination of the tube to the horizontal, degrees
τ	Transmittivity of the glass sheet
a	Represents air
f	Represents fluid
s	Represents metal surface
1	Inner glass tube
2	Outer glass tube

ABSTRACT

A cylindrical solar water heater has been fabricated, theoretically analysed and experimented upon in the present study. The heater consists of two glass tubes of 15.0 and 17.8 cm diameter enclosing a G.I. pipe of 11 cm. diameter. Water is made to flow in the G.I. tube whose outer surface is painted black, which acts as a solar energy absorber.

Experiments have been carried out to test the performance of the water heater under two different modes of operation, namely

- a) natural convection
- b) forced flow condition for mass flow rates of 30, 90, 150 and 210 kg/h.

The day-long collection efficiency under the first mode has been found to be 31.5% while in the second mode it lies between 62 - 77%. The maximum efficiency of 76.4% has been attained for mass flow rate of 150 kg/h.

An approximate theoretical analysis has also been carried out on the heater for forced flow conditions. The experimental results are compared with those obtained theoretically, and the comparison shows a reasonably good degree of agreement.

CHAPTER I

INTRODUCTION

1.1 NEED FOR SOLAR ENERGY UTILIZATION

With the increase in industrialization and advancement of technology there has been an evergrowing demand for energy both in the developed and the underdeveloped countries. To get some idea of the rate of consumption of energy we shall quantify power from 33,000 million tons of soft coal by 'Q' [1]. Until 1850, man had used 9Q. In the next 50 years man had used another 4Q. The present rate of consumption averages to about 10Q per century. By 1980 we shall be using 1Q every five years. This means roughly speaking, that half of all the energy consumed by man in the past 2000 years has been consumed in the last one hundred.

Together with this catastrophe of dwindling fossil fuels, is the tempering of ecological balance of nature because of pollution which comes in the wake of consumption of fossil fuels. Thus there is need to look for alternative sources of inexhaustible and non polluting energy.

Among the alternative energy resources that are being seriously considered at present are : i) Energy from fast breeder reactors, ii) Geothermal energy and iii) Solar Energy. It is believed [2] that if the fast breeder reactor technology

comes through then the existing uranium resources of the world may last another 1,000 years from now. But this has the serious disadvantage of ecological pollution and scientists have still not been able to dispose off radioactive waste safely. Geothermal Energy also offers an alternative to the Energy crisis but at best the stored thermal energy in the world's major geothermal areas would, if completely exploited, provide energy for about 50 years. Even in that time the contribution to the world's annual consumption would be less than that from tidal power which if fully exploited is about 1% of the world's Energy consumption of 1970.

Thus we come to the 3rd alternative i.e. the Solar Energy. It has its own drawbacks like capital cost of equipment etc. but from availability point of view it is inexhaustible and what is more - non polluting. Thus it becomes quite obvious that this Energy be tapped and used for future power needs.

1.2 AVAILABILITY OF SOLAR ENERGY

The amount of Solar Energy incident outside the atmosphere amounts to 1.5×10^{18} kwh/year [3]. But very little of this Energy is available for use by man. Nearly a third of it is lost by reflection to space. Another large fraction is intercepted by the meteorological thermodynamic engine and its associated cloud belts and cloudy regions. Part of it is incident on 70% of earth's surface covered by water. Not all

of what is left of the solar energy is available for human use. Still the amount of energy falling is about 0.2×10^{18} kwh/year which is almost 16,700 times the amount of energy than we now consume [4].

There are two obvious problems in efficiently harnessing solar energy. First, it is not available continuously and thus it necessitates the use of some storage device. Secondly, the energy is diffused in form. While the amount of energy available is enormous, that available at any point is not large enough (solar constant being $2 \text{ Cal/cm}^2\text{-min.}$) to be useful. Thus in order that this energy be of use to man it must be efficiently and economically harnessed.

1.3 HARNESSING OF SOLAR ENERGY

Primarily there are three ways of tapping solar energy, depending upon the form in which we want the output. They are :

- i) Direct Energy Conversion; ii) Concentration of Solar Energy and
- iii) Collection of Solar Energy. The first one is used for directly getting electric power. Its primary use has been in space stations and satellites. The major drawback in such devices has been their low efficiencies like 10 - 15% and very high cost (on the order of Rs. 4 lakhs/kw). The second method, namely the concentration of solar energy is used for getting high temperatures e.g. for generating steam to run pumps or generate power or to use it for studying high temperature technology. Fresnel

lenses and parabolic concentrators are normally used for this purpose. The major drawback in these types of concentrators is the difficulty in making them, their high cost and the rather complicated system needed to make them track the sun. The third method, viz. the collection of solar energy is the cheapest and the easiest way of tapping this energy, particularly where the requirement of temperatures is of the order of 100°C . Apart from their usage in space heating or cooling, water distillation and fruit drying, their maximum use has been for solar water heating. This can be used in western countries and in some northern regions of India in winter. Apart from this usage, the development of these collectors is useful for a country like India from the point of view of making an efficient device for generating steam or evaporating a liquid of low boiling point which in turn will drive a pump. Recently Mienel and Mienel [5] have found that it is feasible as well as 'economical' to use flat plate selectively absorbing collectors to generate power on a large scale. They envisage the total collecting area of $118 \times 118 \text{ km}^2$ which will generate 10^6 megawatts. Secondly these sort of collectors can be used as generators for absorption type of refrigeration cycle. Thus to start with there is a need to develop efficient solar water heater.

1.4 REVIEW OF PREVIOUS WORK

[Since maximum work has been done in solar water heating, the literature abounds in different types of heaters.] These

heaters differ from one another on minor points but they can broadly be classified into three categories. These are :

i) Tube type heater :

This is the most common type of heater. Its cross section is shown in Fig. 1.1

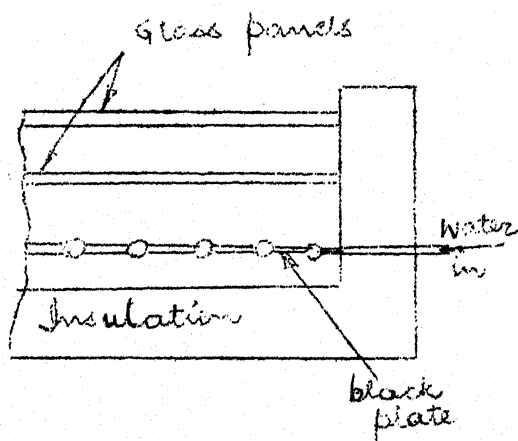


Fig. 1.1

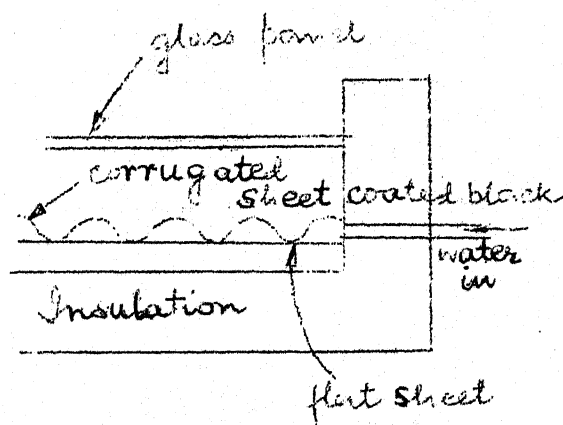


Fig. 1.2

Yellot and Sobotka [6] have investigated the performance of this type of solar water heater. The steel pipes are simply pressed into thermal contact with the absorbing plate. The absorbing plate was coated with a selectively absorbing coating as developed by Tabor [7]. There were 2 glass covers. The collector area was 2.8 m^2 and steel pipes were of 12 m.m. diameter. They have reported an efficiency of 38.5% for the whole day (natural convection). For flow rates of 44.5 kg/h and 84 kg/h the average daily collection efficiency was 44.3% and 45.5% respectively.

ii) Corrugated sheet type heater

The heater, Fig. 1.2, consists of a corrugated sheet, coated with black paint, attached to a flat sheet by means of rivets. Water flows in the 'pipes' formed by the sheets. Rao and Suri [8] have experimented with this type of heater. For a collector surface area of 2.32 m^2 and the tank capacity of 136 litres the rise in temperature of water in winter at Roorkee, in natural circulation, was from 6°C to 50°C (max.). The efficiency was found to be 63%. The major problem in such type of heaters is the leakage from the riveted joints.

iii) Heater cum storage type

These types of heaters do away with the storage tanks. The heater acts as both. Thus the cost is considerably reduced in this case. Chinappa and Gnanalingam [9] have made and tested one such heater. The heater consists of a square coil of 7.55 cm diameter and 13.5 m. long in a wooden box with insulation at bottom and 2 glass covers. Glass surface area is 1.86 m^2 . By drawing off water when its temperature reaches 49°C , it is possible to obtain 136 - 230 litres of water/day. The collector efficiency has been found to be 46%.

Another type of built-in storage water heater has been built and tested at Central Arid Zone Research Institute, Jodhpur by Garg and Krishnan [10] . The heater consists of a galvanised iron (20 gauge) rectangular tank of dimensions $112 \times 80 \times 10 \text{ cm}$

with a capacity of about 90 litres. This tank is placed in a rectangular mild sheet tray and insulated from sides and back. In front is ordinary glass. The front face of the tank is blackened by lamp black paint. Water temperatures of 55 °C have been reported for winter. The efficiency of this type of heater has been reported as 75%.

Chauhan [11] has also built almost the same type of heater as above. The capacity of this heater is 70 litres. The maximum temperature attained in the month of April has been 86 °C at about 3.30 p.m. The collector efficiency of 72% has been reported in the forced flow conditions with the mass flow rate of 76 kg/hr. In the natural convection mode the collector efficiency has been found to be between 50 - 58%.

1.5 MOTIVATION FOR THE PRESENT WORK

There are certain disadvantages with the types of solar heaters cited above. One of the important disadvantages is the flat surface of the collector itself. Set at a specified angle of inclination, the surface receives an effective sunbeam, the width of which varies between zero and that of the collector during the day, as the sun's position in the sky changes. In addition, there exists many avenues for energy losses due to :

- i) conduction from the back and edges of plate,
requiring heavy insulation for minimization,

- ii) Radiation and convection from the flat - plate surface and the water tubes,
- iii) Reflection from and absorption by glass covers, caused by variation in the angle of solar incidence, and
- iv) Conduction through the insulation surrounding the pipes connecting the collector and the water tank.

As a result of these losses, the average yearly collector efficiency is between 30 - 40%. In order to improve the collector efficiency, a cylindrical solar water heater, using a cylindrical surface has been fabricated and investigated by Vincze [12]. The collector is a tube painted black and covered by 2 glass tubes with 2.5 cm space between them. The capacity of heater is 22.2 l and the projected area is 0.186 m^2 . When placed at an angle of 63° to the horizontal temperatures as high as 58°C have been reached during the month of August. Vincze has reported efficiencies of the order of 216%. The reason for such high efficiency is given in Chapter IV. The water is in the natural circulation.

As the efficiency appears to be very high it has been thought appropriate to investigate this type of heater more thoroughly, especially since it appears to be a very good answer for airconditioning devices driven by solar energy.

The most important advantage of this type of collector is that the effective beam width for incident radiation remains equal to the tube diameter over all the sunshine hours of the day. Moreover losses due to conduction at the edges are negligible, since the area for axial energy conduction is small compared with the tube surface and may be well insulated.

Thus in the present work a solar water heater of cylindrical type has been fabricated. It consists of a G.I. tube of 10.15 cm bore and 11 cm outer diameter coated with lamp black paint. The tube is surrounded by 2 glass tubes of Pyrex glass of diameters 15.0 and 17.8 cms. respectively. The capacity of the heater is 22.45 litres. The heated section is 1.2 m long.

The heater has been tested for different mass flow rates of water starting from 0.5 kg/min to 3.5 kg/min. It has also been tested for natural circulation. The difference between the inlet and outlet temperatures of the water has been noted for the whole day and efficiencies have been calculated. The efficiencies have been found to lie between 62 - 77% for different mass flow rates in the range of experimental data.

An approximate theoretical analysis on this heater has also been carried out and the results are compared with those obtained experimentally.

CHAPTER II

THEORETICAL ANALYSIS

The cylindrical solar water heater under analysis, is as shown in Fig. 2.1. It consists of a metallic tube, which has been assumed to be coated with a selectively absorbing coating [7], placed coaxially between two cylindrical shells of glass, which act as energy shields. Each inner tube diameter is assumed to be $\sqrt{3}/2$ of that of the tube immediately surrounding it, so that most of the radiation transmitted by the outer tube may be incident on the inner tube. The axis of the tube is maintained at an appropriate angle of tilt in the North - South direction, to effect normal solar - radiation incidence at noon time, on the design day. Water is forced to flow at a constant rate through the metallic tube by some external means.

It is clear that the total incident intensity of radiation on the tube surface, q , varies with time of the day. As a result, the temperature of the metallic tube at any section is expected to vary circumferentially as a function of time. In order to reduce the complications that will be introduced in the analysis of the temporal and circumferential variations in solar energy input, it has been assumed that the total radiation incident on the tube surface remains constant at a value equal to the average intensity during the sunshine hours, for the place under

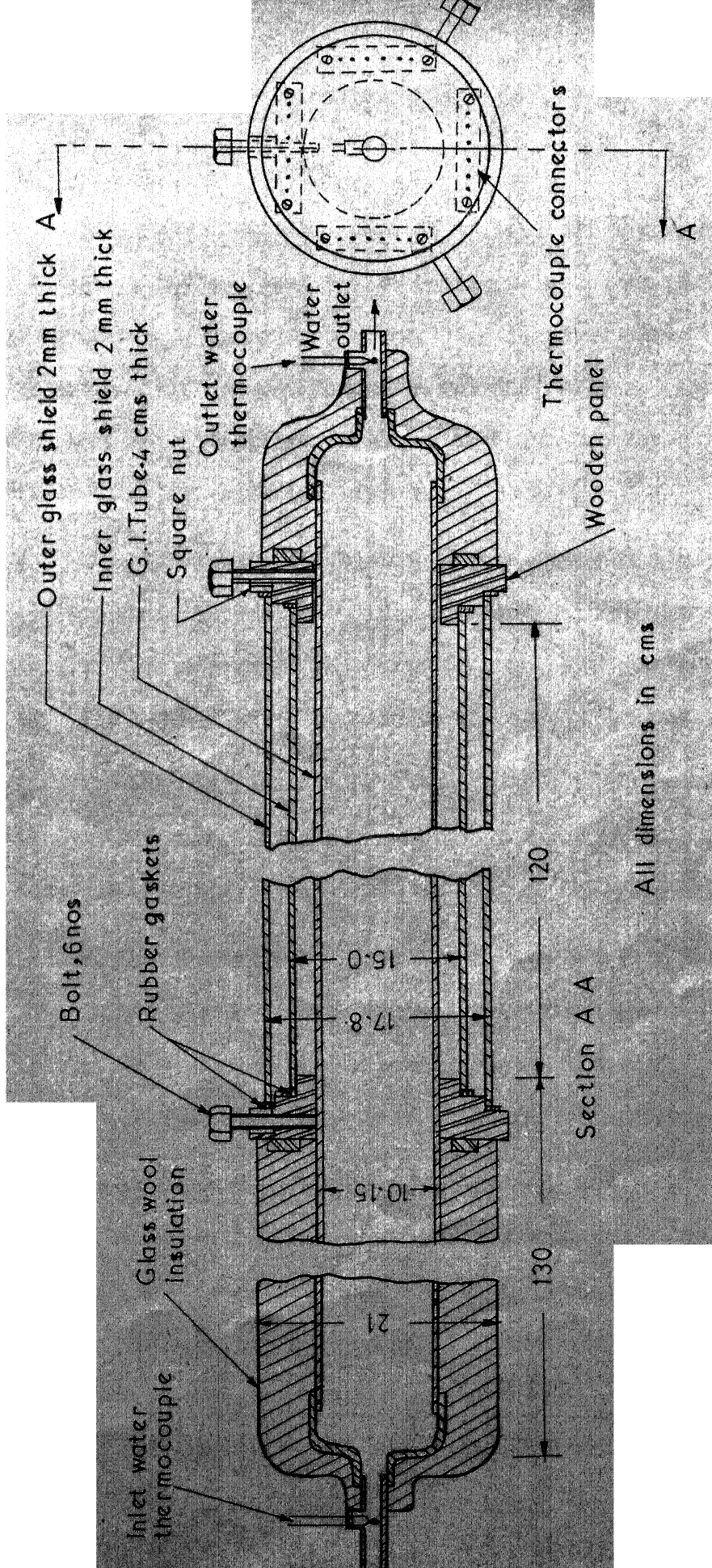


FIG. 2.1 SECTIONAL VIEW OF THE APPARATUS.

consideration. This assumption permits us to treat the system as one in steady state. Further, the average intensity is assumed to be due to a combination of the effects of direct solar radiation, diffuse sky radiation and the reflected ground and other long wave length radiations. The equations used in this calculation are exhibited later on.

Since the transmittivity and absorptivity of glass vary with the angle of incidence of the radiation, average values of these quantities, assumed to remain constant over the whole periphery of the glass shields, have to be used in the analysis.

With the simplifications listed above, it is possible to write down the energy balance equations for the whole system. A few other simplifying assumptions used in the analysis are :

- i) The thermal conductivities of the metallic tube and glass surfaces are sufficiently high and the tube thicknesses so small, that the thermal resistances due to the three walls may be neglected;
- ii) Axial conduction through the fluid and the metallic tube is negligible, since the product, $Re Pr$ (Re = Reynold's number based on the tube diameter and the mean velocity of the flow through the tube, Pr = Prandtl number for fluid) is large, being 1280 for lowest mass flow rate of 0.5 kg/min. and the wall thickness is small;

- iii) Conduction losses from the ends of the tubes are negligible, since the diameter of the outermost glass tube is small compared with the solar water heater length and the ends are well insulated, and
- iv) The fluid properties are invariant in temperature because of the small temperature range involved in the heating process. Moreover, the viscous dissipation effects have been neglected in the formulation of energy balances because of the small velocity gradients involved.

2.1 ENERGY BALANCE EQUATIONS

Considering the outer glass tube, it is seen that the tube receives energy due to irradiation from the surroundings and due to convective as well as radiative energy exchanges with the inner glass tube. It loses energy to the environment through convection and radiation.

An energy balance on the outer glass tube therefore yields :

$$\begin{aligned}
 D_1 U_{1-2} (T_1 - T_2) + \sigma F_{1-2} D_1 (T_1^4 - T_2^4) + \alpha_2 D_2 q \\
 = h_a D_2 (T_2 - T_a) + \epsilon D_2 \xi_2 (T_2^4 - T_a^4)
 \end{aligned} \quad (1)$$

where D_1 and D_2 are respectively the diameters of the inner and outer glass tubes, U_{1-2} is the overall heat transfer coefficient

between the outer and inner glass tubes and F_{1-2} is the view factor for radiation between the inner and outer glass shields. The temperatures of the inner and outer glass shields, respectively, are T_1 and T_2 , while h_a , is the heat transfer coefficient between the outer cylinder of glass and the ambient air and T_a is the ambient temperature. The term σ , is the Stefan - Boltzman constant. The quantities α_2 and ϵ_2 are respectively the absorptivity and emissivity of the outer glass surface for solar radiation and long wave length radiation.

For inner glass tube, similar considerations of energy balance yield :

$$\begin{aligned}
 D_1 U_{1-2} (T_1 - T_2) + \sigma F_{1-2} D_1 (T_1^4 - T_2^4) \\
 = \alpha_1 \epsilon_2 D_1 q + D_s U_{s-1} (T_s - T_1) + \\
 + \sigma D_s F_{s-1} (T_s^4 - T_1^4) \quad (2)
 \end{aligned}$$

where α_1 and ϵ_2 are respectively the absorptivity and transmittivity of the inner and outer glass shields, D_s is the metal tube diameter, U_{s-1} is the overall heat transfer coefficient between the metal tube and the inner glass tube and F_{s-1} is the view factor for radiation between the metal tube surface and the inner glass tube.

In writing Eqs. (1) and (2) inter-reflections between the inner and outer glass tubes have been considered as small and

neglected. Neglect of these interreflections tends to increase the apparent energy losses from the metal tube surface, and hence gives a conservative estimate for solar heater efficiency.

Since the liquid flowing into the tube is one of relatively high Prandtl number ($4 < \text{Pr} < 6$), it has been assumed that the velocity profile is fully developed at the entry of the heated section, permitting use of the thermal entry length solution for arbitrary wall energy flux [13]. For the tube surface temperature T_s we can therefore write the equation :

$$T_s(x^*) - T_e = \left[D_s / (2 k_f) \right] \int_0^{x^*} g(x^* - \xi) q_0(\xi) d\xi \quad (3)$$

where,

$$g(x^*) = 4 + \sum_{nn} \exp(-\gamma_n^2 x^*) / (\gamma_n^2 A_n) \quad (4)$$

and

$$q_0(x^*) = \tau q - U_{s-1} (T_s - T_1) - \sigma F_{s-1} (T_s^4 - T_1^4) \quad (5)$$

represents the effective energy flux absorbed by the metal tube surface, assuming that the absorptivity is unity. In Eqs. (3), (4) and (5), T_e is the fluid temperature at the tube inlet and x^* is a non dimensionalized axial coordinate measured from the tube inlet, given by the equation

$$x^* = 2x / (D_s \text{Re} \text{Pr}) \quad (6)$$

On differentiating eq. (3) with respect to x^* and using the rule for differentiation under the integral sign [14], we obtain,

$$(2 k_f / D_s) d T_s / d x^* = \int_0^{x^*} (d / d x^*) g (x^* - \xi) q_0 (\xi) d \xi + g (0) q_0 (x^*) \quad (7)$$

If we now substitute for $g (x^* - \xi)$ and $q_0 (x^*)$ from eqs. (4) and (5) into the above and use the integral mean value theorem [15], we obtain :

$$\begin{aligned} (2 k_f / D_s) d T_s / d x^* = & \left[C_1 \left\{ T_q - U_{s-1} (T_s (\bar{x}^*) - T_1 (\bar{x}^*)) \right. \right. \\ & - \sigma F_{s-1} \left[T_s^4 (\bar{x}^*) - T_1^4 (\bar{x}^*) \right] \left. \right\} + C_2 \left\{ T_q - U_{s-1} \right. \\ & \left. (T_s (\bar{x}^*) - T_1 (\bar{x}^*)) - \sigma F_{s-1} \left[T_s^4 (x^*) - T_1^4 (x^*) \right] \right\} \right] \end{aligned} \quad (8)$$

where,

$$C_1 = \sum_n \left[\exp (-\gamma_n^2 x^*) - 1 \right] / (\gamma_n^2 A_n) \quad (9)$$

and

$$C_2 = 4 + \sum_n 1 / (\gamma_n^2 A_n) \quad (10)$$

while \bar{x}^* , represents a point in the interval $0 < \bar{x}^* < x^*$, at which the various temperatures are to be evaluated. Further, in eqs. (4), (9) and (10), the quantities γ_n are eigen values and the quantities A_n are constants, listed in [13].

The mixed mean temperature, T_m , of the fluid flowing through the tube is given by equation; [13]

$$d T_m / d x^* = (2 D_s / k_f) q_0 (x^*) \quad (11)$$

k_f being the fluid thermal conductivity.

If eqs. (2), (3), (8) and (11) are now solved simultaneously to determine the temperatures, T_1 , T_2 , T_s and T_m , as functions of x , we can evaluate the heater efficiency (between the inlet and the point under consideration) by writing :

$$\eta = \dot{m} c_p (T_m(x) - T_e) / (D_2 \times q) \quad (12)$$

where \dot{m} , is the mass flow rate of fluid flowing through the tube, and T_e is the entry temperature of the fluid.

2.2 EVALUATION OF CONSTANTS AND HEAT FLUX q

Before the solution of the above equations be attempted it is necessary to find the constants like U_{1-s} , U_{1-2} , F_{1-s} , F_{1-2} etc and the solar radiation input. We shall calculate each of these one by one.

Solar Energy Radiation Input q

The total radiation falling on a horizontal plane at I.I.T. Kanpur has been recorded for every day by the Civil Engineering Department on the pyranometer supplied by Indian Meteorological Department. Graphs have been taken from them both for direct and diffuse radiation.

The total radiation on the collector consists of;

- i) direct radiation on the top surface, ii) diffuse sky radiation on the top surface and iii) ground reflected radiation on the bottom surface.

The heater is inclined to the horizontal at an angle calculated from the equations : [16]

$$\begin{aligned}\sin \beta &= \cos L \cos \delta \cos H + \sin L \sin \delta \\ \sin \phi &= \cos \delta \sin H / \cos \beta, \quad \text{and} \\ \cos \theta &= \cos \beta \cos \phi \sin \psi + \sin \beta \cos \psi\end{aligned}\quad (13)$$

where L = latitude angle; for Kanpur it is $26^{\circ}26'$, δ = declination angle and H = hour angle = $54'$. The sunshine hours are taken to be from 7 AM to 5 PM. It has been assumed that the declination angle changes very little between 29th May to June 12 (test dates), ranging between 21° and 23° . Thus the average angle has been taken to be 22° .

Assuming that the direct solar radiation should be normal to the tube axis at 12 noon for maximum utilization on the design day (i.e. $\theta = 0$ or $\cos \theta = 1$), the equations above yield;

$$\psi = 6^{\circ}$$

which is the inclination of the tube to the horizontal.

Thus the direct normal radiation, as seen from the graph of insolation, be multiplied by $1/\cos \psi$ to make it normal on the inclined surface.

The diffuse radiation falling on the inclined surface should be multiplied by a factor : [17]

$$R_s = (1 + \cos \psi) / 2$$

so as to make it normal on the inclined surface.

The ground reflected radiation, falling only on the under side of the heater, is found as follows :

$$R_{GR} = (R_{DN} + R_{Df}) F_D r_g ,$$

where R_{DN} = Direct normal radiation, R_{Df} = normal diffuse radiation, F_D = shape factor between the ground and the heater = .81 and r_g = ground reflectance = .12 for gravel roof top. [18]

The total radiation, for the day of experiment, falling on the heater can thus be calculated as :

- i) Direct radiation : This radiation is assumed to fall only on the projected area formed by an arc of 120° of the cylinder. The rest gets all reflected from the surface. This area for the heater is 0.186 m^2 .
- ii) Diffuse radiation is assumed to fall only on the upper portion and the projected area is 0.214 m^2
- iii) Ground reflected reflection is assumed to fall only on the under side of the collector and the projected area is 0.214 m^2 .

Overall Heat Transfer Coefficients

The overall heat transfer coefficients, U_{1-2} and U_{s-1} , appearing in eqs. (2), (3) and (8), have to be obtained from the curves on overall film conductances for free convection flow

between concentric cylinders provided by Jakob [19]. Under the conditions of the present computations where $D_2 = (2 / \sqrt{3}) D_1 = (4/3) D_s$, the overall film coefficients are very nearly equal to the respective thermal resistances caused by the presence of annular air gaps, we can therefore write for U_{1-2} and U_{s-1} the approximate equations ;

$$D_1 U_{1-2} = 2 k_a / \ln (D_2 / D_1), \text{ and } D_s U_{s-1} = 2 k_a / \ln (D_1 / D_s) \quad (15)$$

Outside Heat Transfer Coefficient

Assuming the average wind velocity of 12.15 km/h in the East-West direction for Kanpur [20] the heat transfer coefficient h_a , between the outside air and outer glass shield of diameter, D_2 can be calculated by using the equation: [21]

$$\frac{h_a D_2}{k_a} = a (Re)^b$$

where k_a is the thermal conductivity of the ambient air and the Reynold's number, Re is based on the outer tube diameter and the design wind velocity. The quantities, a and b , are constants which depend upon Reynold's number. The value of h_a , calculated in this manner comes out to be $15 \text{ kcal/hr} - \text{m}^2 - ^\circ\text{C}$.

Shape Factors

The calculations involve shape factors for a system of two concentric and coaxial cylinders, where the inner surface of the outer cylinder radiates to itself. Shape factors for this

case has been presented in the form of graphs by Hottel and Sarofim [22] and have been used in the present calculations. A knowledge of these shape factors enables the determination of F_{1-2} and F_{s-1} , appearing in Eqs. (2), (3) and (8), by the use of standard expressions for radiant energy exchange between coaxial cylinders with gray inner surfaces [22]. The values of F_{1-2} and F_{s-1} calculated in this way are :

$$F_{1-2} = 0.802, \text{ and } F_{s-1} = 0.895.$$

The values of transmittivities, absorptivities and emissivities of glass and metal surface (with a selectively absorbing black coating), are listed below in Table 2-1.

TABLE 2-1

Transmittivities, Absorptivities & Emissivities [7]

Surface		Solar		Normal	
		τ	α	α	ϵ
Glass	Single	0.88	0.05	0.06	0.94
	Double	0.81	-	-	-
Metal Tube		0.0	1.0	0.91	0.09

2.3 METHOD OF SOLUTION

The coupled and non linear differential equations involved in the determination of T_1 , T_2 , T_s and T_m , preclude the possibility of obtaining analytical solutions. The simplest mode

of attack is therefore to obtain numerical solutions for parametric values of the tube diameter, D_s , the mass flow rate, \dot{m} and the tube length. Using the data as specified above along with the specified diameters which are 11 cms, 15 cm and 17.8 cm for metallic tube, inner glass shield and outer glass shield respectively, and the mass flow rate of the liquid through the tube, an iterative, step-by-step calculation may be carried out. The steps involved in the computation are the following :

- a) Choosing a sufficiently small x , say 1 cm., and assuming the metal surface at the inlet, equal to that of the entering water, the simultaneous equations for T_1 and T_2 at the inlet are determined numerically. The technique used in the calculations is Newton's method of tangents, assuming that the initial guesses are sufficiently close to the roots [23].
- b) Using Eqs. (2) - (8) as well as T_1 and T_2 as determined above, a first estimate of $T_s \{ x^* \}$ is obtained. In this calculation it has been assumed that \bar{x}^* is approximately equal to $x^*/2$, since x^* is small ($13.9 \times 10^{-5} / \dot{m}$) and there is not likely to be much of difference between \bar{x}^* and $x^* / 2$.
- c) After setting $T_s \{ x^* / 2 \} = T_s (0) + T_s \{ x^* \} / 2$, steps (a) and (b), are repeated until the newly computed values of $T_s \{ x^* \}$ agrees with that computed early closely. The values of T_1 , and T_2 corresponding to $T_s \{ x^* / 2 \}$ and $T_s \{ x^* \}$ as well as the liquid temperature, $T_m \{ x^* \}$ are determined by using the appropriate equations.

- d) The efficiency of the solar water heater in the interval 0 to x is

$$\eta = \dot{m} c_p (T_m \leftarrow x^* \rightarrow - T_e) / (D_2 q x)^* \quad (16)$$

- e) Now, the origin may be translated to the point $x = x^*/2$, so that the new starting values for the computations are $T_s(0) = T_s \leftarrow x^*/2 \rightarrow$, $T_1(0) = T_1(x^*/2)$ and $T_2(0) = T_2(x^*/2)$. The calculations at steps (b), (c) and (d) are repeated, until the temperatures along the tube surface as well as the mixed mean fluid temperatures, and the efficiencies at all values of x, are obtained.

The computer programme to evaluate the temperatures using the above scheme is listed in Appendix I.

The computations may be stopped, once the end of the tube is reached which is 1.20 m in the present set up. However, if the purpose of the calculation is to determine the solar heater length needed for maximum energy collection when the tube diameter and the mass flow rate are specified, it is necessary to continue the calculations until the newly computed fluid temperatures $T_m \leftarrow x^* \rightarrow$ does not differ appreciably from that one step computed earlier. For the tube diameter of 18 cms and mass flow rates of 0.5, 1.5, 2.5, 3.5, 4.5, 5.5 and 6.5 kg/min. the optimum length has been found [24]. For mass flow rate of 0.5 kg/min. the optimum length comes out to be 6 m, the difference between T_m at 6 m and that at 7 m being less than 2%.

In the present work the computations have been done for mass flow rates of 0.5, 1.5, 2.5 and 3.5 kg/min. The comparison of results between those computed and found experimentally are shown in Fig. 4.6.

* This expression is not valid for natural convection case. The efficiency of heater in the natural convection mode is:

$$\eta = m c_p (T_f - T_i) / Q$$

where m = total amount of water in the heater

T_f = Temperature of water at the end of day

T_i = Temperature of water in the morning

Q = Total radiation (direct, diffuse and ground reflected) incident on the heater during the day.

CHAPTER III

EXPERIMENTAL SET UP

In order to check the theory and also to study cylindrical solar water heaters more thoroughly, a heater has been fabricated and experimented upon. The line diagram of the set up is shown in Fig. 3.1. The main parts of the set up will be described under two headings, i) Apparatus and ii) Instrumentation.

3.1 APPARATUS

i) G.I. Tube

A tube 2.5 m long, 10.15 cm. inner diameter, and outer diameter 11 cm., made of Galvanised Iron is used for heating the water. In the theoretical analysis of the heater it has been assumed that the flow of water in the tube is fully developed. Hence a sufficiently long entry length must be provided at the tube inlet to ensure a fully developed flow.

The hydrodynamical entry length can be calculated by using the equation : [25]

$$x = 0.03 \text{ Re } D$$

where x = entry length, Re = Reynolds number and D = diameter of the tube. The mass flow rates for which the heater has been experimented upon vary from 0.5 kg/min to 3.5 kg/min.. For 3.5 kg/min. mass flow rate, the entry length comes to 3.2 m. Since such a long tube was not available the longest tube available, which is 2.5 m long has been used.

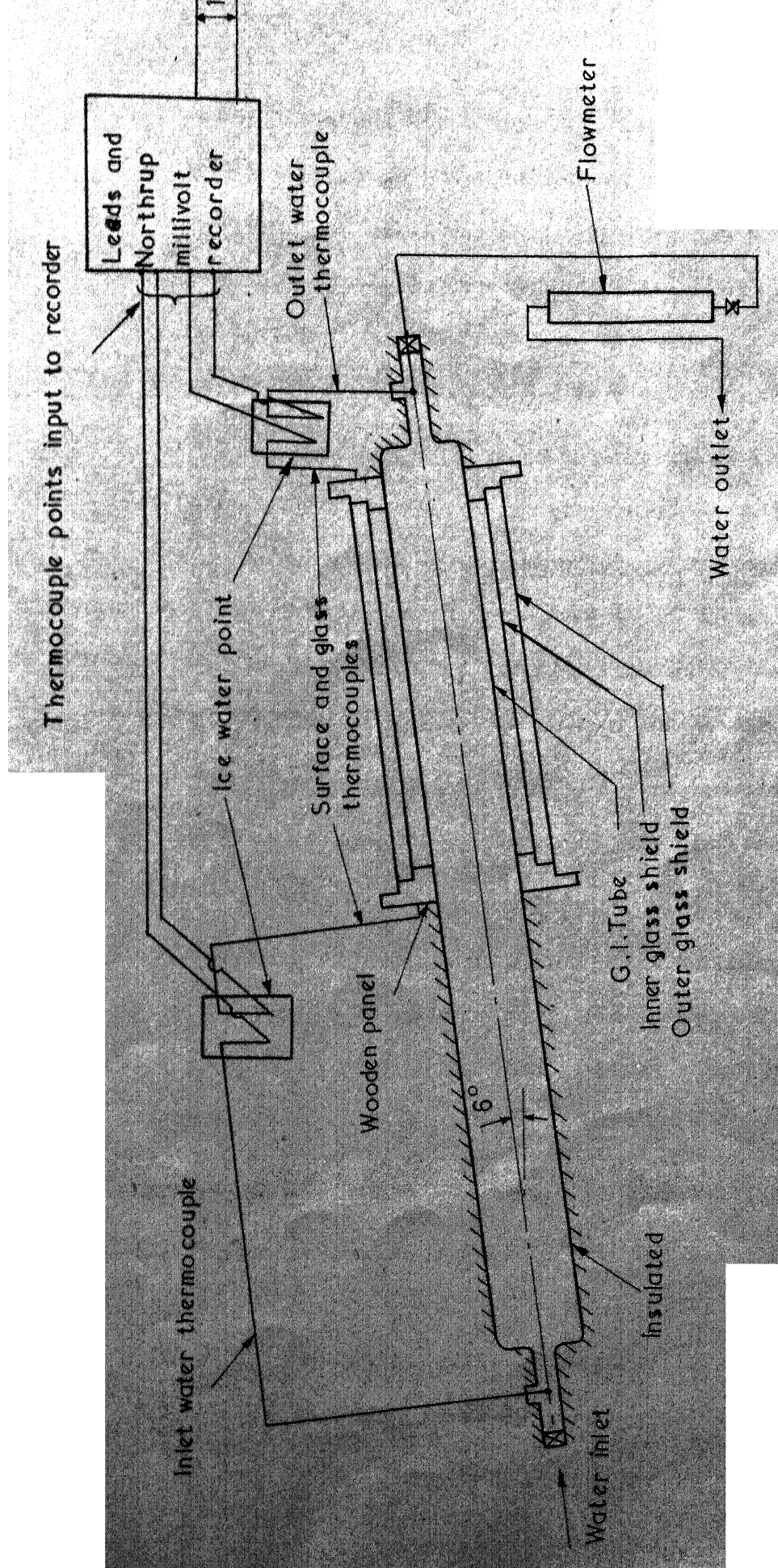


FIG. 3.1 LINE DIAGRAM OF THE EXPERIMENTAL SET UP

The heated section of the tube is 1.2 m. Thus the remaining 1.3 m length of the tube acts as the entry length. For mass flow rates of 0.5 kg/min. and 1.5 kg/min. the entry length as found by equation above comes to 0.45 m and 1.35 m respectively. Thus fully developed flow as assumed in the theory can exist only for flow rates of 0.5 kg/min. and 1.5 kg/min....

Since this length is meant only for developing the flow, it has been insulated by 5 cm thick glass wool so that sun does not heat up this portion. By making simple calculations it has also been seen that the amount of energy input in this section, because of direct, diffuse and ground reflected radiation, comes out to be less than 1% of that incident on the heated section.

The portion of the tube to be heated has been painted black with a paint which is a mixture of lamp black and black enamel paint.

Water is allowed to flow from the lower end of the tube which is inclined at an angle of 6° to the horizontal, as shown in Fig. 3.1. The flow rate has been measured with the help of a flow meter.

ii) Wooden Panels

These panels are mounted on the tube and clamped to it by means of 6 bolts, 3 on each one of them, as shown in Fig. 2.1. At the back of these panels are the thermocouple wire connectors.

In order that the connectors are not exposed to sun they have been shaded by white packaging material.

iii.) Glass Shields

The two glass shields are of 15.0 and 17.8 cm diameter respectively. They are made of pyrex glass with average transmittivity of 0.89. The glass shields are 2 mm thick. The air gap between the G.I. tube and two glass shields is 2 cm and 1.5 cm respectively. These shields are mounted on steps made on the wooden panels, as shown in Fig. 2.1. Rubber gaskets have been placed at the rim of the panel so that contact between glass shield and panel is good, thus preventing any entrance of dust or dew.

3.2 INSTRUMENTATION

i) Temperature Measurements

The temperatures of water as well as the G.I. tube and glass shields have been measured by calibrated 24 gauge insulated copper constantan thermocouples. 16 thermocouples have been soldered to the tube as shown in Fig. 3.2, while 5 thermocouples

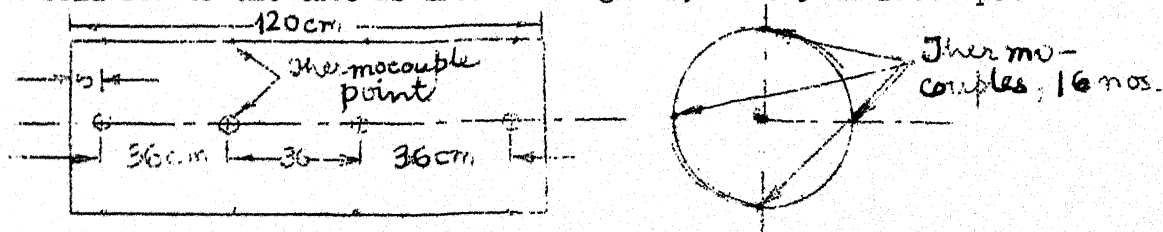


Fig 3.2

are fixed on outer and inner glass shields by means of an adhesive, epoxy resin.

The water inlet and outlet temperatures have been measured by dipping the thermocouples in inlet and the outlet pipes as shown in Fig. 3-1.

The ambient temperature has been measured by putting a thermometer, with a least count of 0.1°C , in shade.

ii) Recorder

A Leeds and Northrup millivolt recorder with a least count of 0.05 mV has been used to record the temperatures.

iii) Solar Radiation Measurements

Solar radiation has been measured by Epply^c pyranometer installed by National Meteorological Laboratory Poona at the Civil Engineering Department of I.I.T. Kanpur. The charts from this recorder for both direct and diffuse radiation have been used to calculate the amount of radiation falling on the solar water heater. The radiation as read from these charts is that incident on a horizontal surface. The radiation incident on an inclined surface corresponding to the inclination has been calculated therefrom by using appropriate factors as shown in Chapter II.

3.3 MODES OF TEST

The performance of the heater has been tested under two conditions :

- i) Natural circulation
- ii) Forced circulation

Natural Circulation

In this mode, the pipe is filled with water in the morning and the tap at the lower end of the tube is closed. The temperatures of the tube and the glass shields are recorded. At the end of the day, the inlet and the outlet of the tube are connected by a small pump (0.025 hp) through polythene pipes so that the water is thoroughly mixed. The final temperature of the water is then recorded.

Forced Circulation

The water is forced in the tube from below. There is no use of pump as the tap pressure is enough to force the water to the maximum flow rate of 3.5 litres/min. Temperatures both for inlet and outlet water as well as those of the tube and the glass shields are measured. At the end of the day the water in the tube is mixed by the pump in order to measure the total thermal energy gained by the system. The heater has been tested for four mass flow rates, 0.5, 1.5, 2.5 and 3.5 kg./min..

CHAPTER IV

RESULTS AND DISCUSSIONS

4.1 RESULTS

The experimental phase of this study consisted of tests conducted during the months of May and June, 1974. During the test period, a wide range of climatic conditions were encountered; particularly the onset of early monsoon made it difficult to carry out tests on all days. Thus only the data obtained on the days when there was uninterrupted sunshine is presented in this work.

The heater was tested in two modes viz. natural convection and forced convection. Table 4.1 shows the experimental data and results for natural convection.

Table 4.1 : Experimental Data and Results for Test in Natural Convection (May 18, 1974).

Water temperature °C		Time		Tilt angle	Insolation (kcal)			Heat gained by water (kcal)	Effi- ciency %
Initial	Final	From A.M.	To P.M.		Direct	Diffuse	Ground reflected		
34.5	55.3	7.20	6.10	8°	1040	487.15	172.5	535	31.5

Figure 4.1 shows the plot of the experimental data for natural convection. The direct and diffuse solar radiation falling on the tilted collector are plotted, together with the plate temperature and the ambient temperature. The maximum plate temperature of 63.5 °C was obtained at 3.00 p.m. after which it started

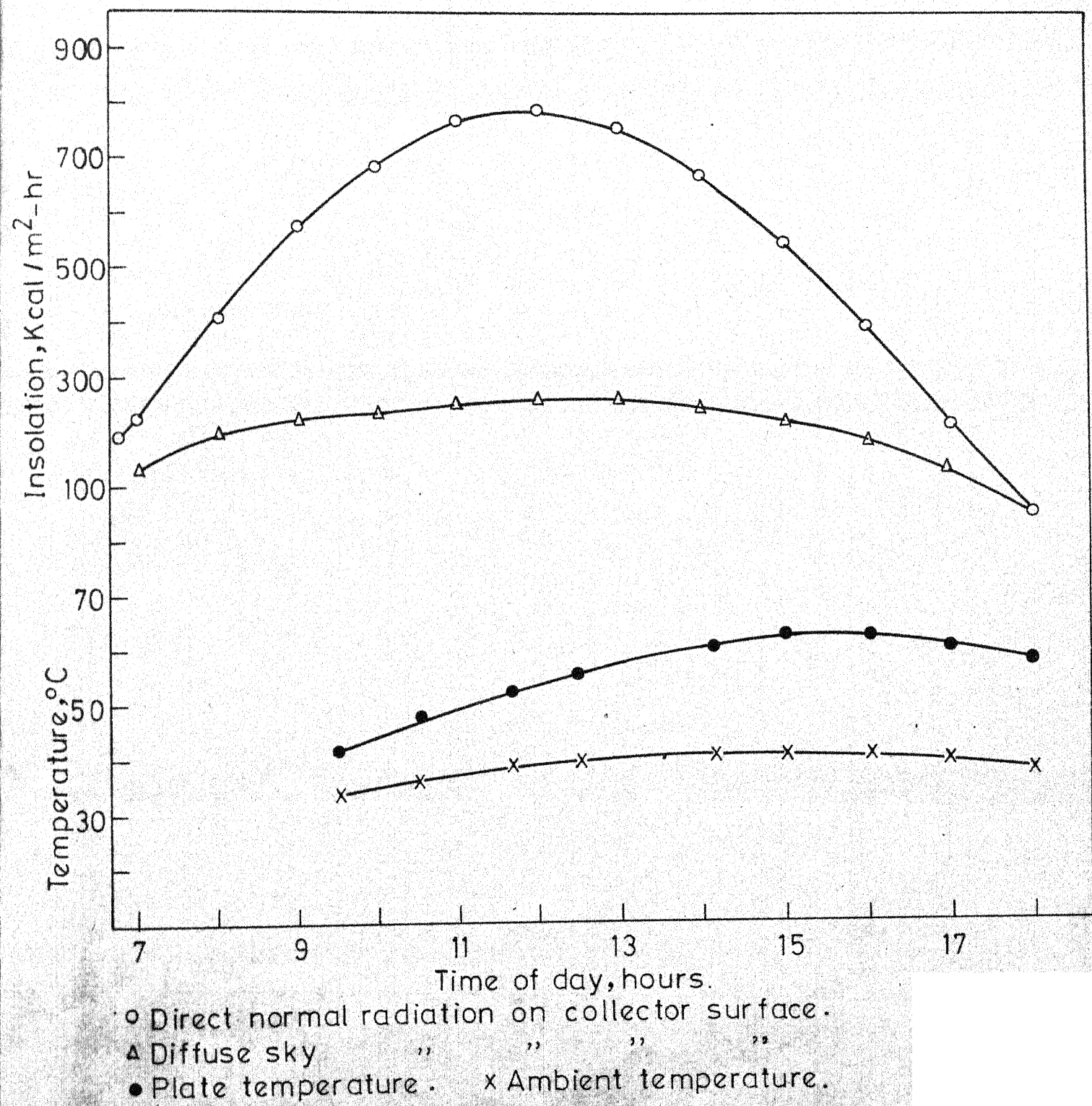


FIG.4.1 Experimental results for test at Kanpur, May, 18 1974 for natural circulation.

to decrease since the heat losses from the plate to the surroundings were more than the input by solar radiation.

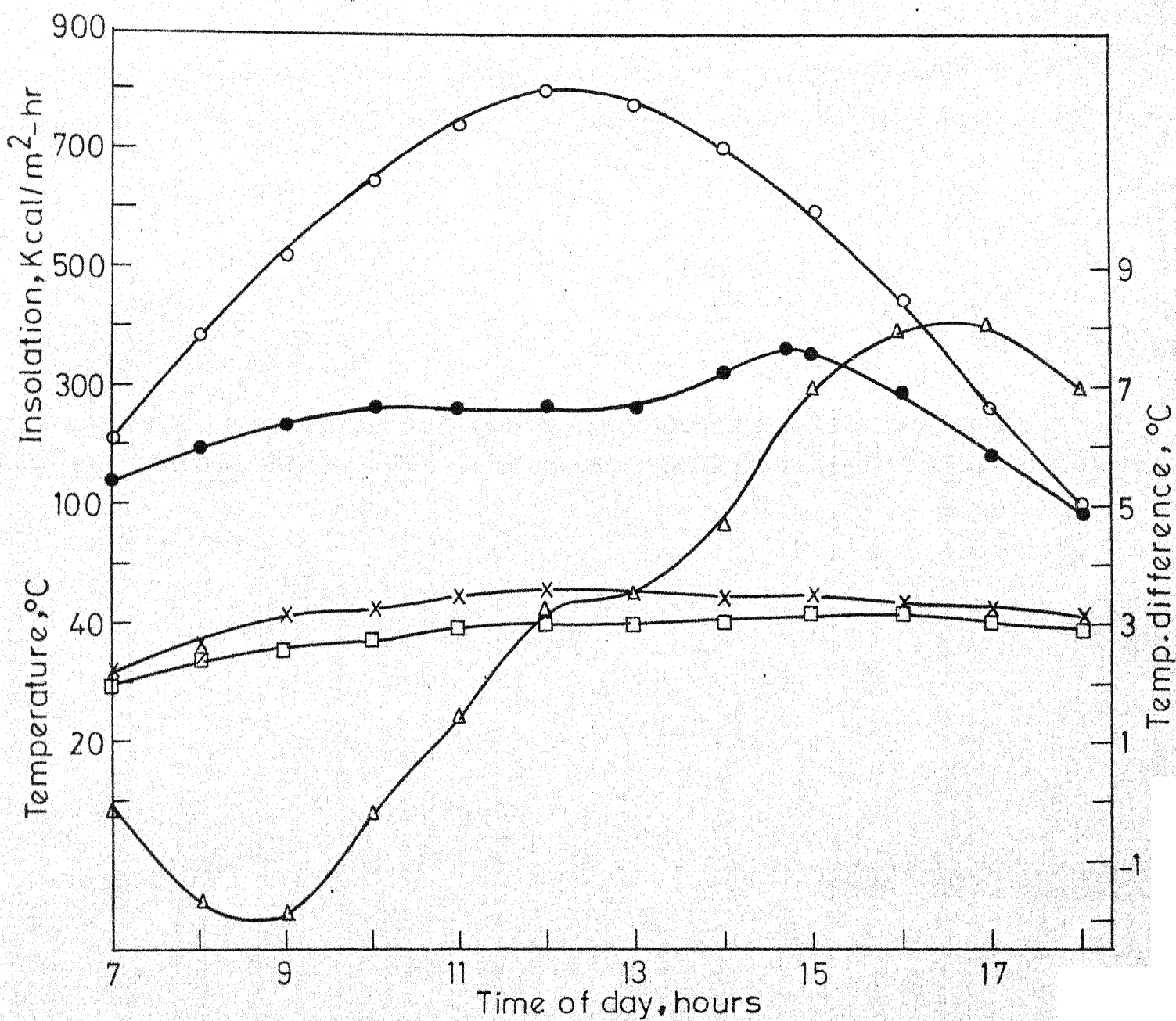
The efficiency obtained in this case is rather small being 31.5%. A possible reason is that since the angle of tilt of the heater to the horizontal is small (8°), convection currents do not develop readily. Also since the upper surface of the tube is heated there is no radial convection. More vigorous convection could have been obtained if the angle of tilt had been around 30° , but then this would have been at the expense of less solar input to the heater, because then the solar input would not have been normal to the surface of the heater.

Since the efficiency in natural convection is small a better indication of the effectiveness of the heater would be to test it under forced convection. This does not mean that the efficiency of such a type of heater will be small in natural convection, but it simply means that under the conditions of present experiment when the inclination angle is 8° , it will be small. Table 4.2 tabulates the results for test in continuous flow for different mass flow rates.

Figures 4.2 - 4.5 show the plot of experimental results for forced convection. Together with the total radiation falling on the heater, the outer glass temperature and the difference between the water temperatures at the outlet and the inlet are plotted.

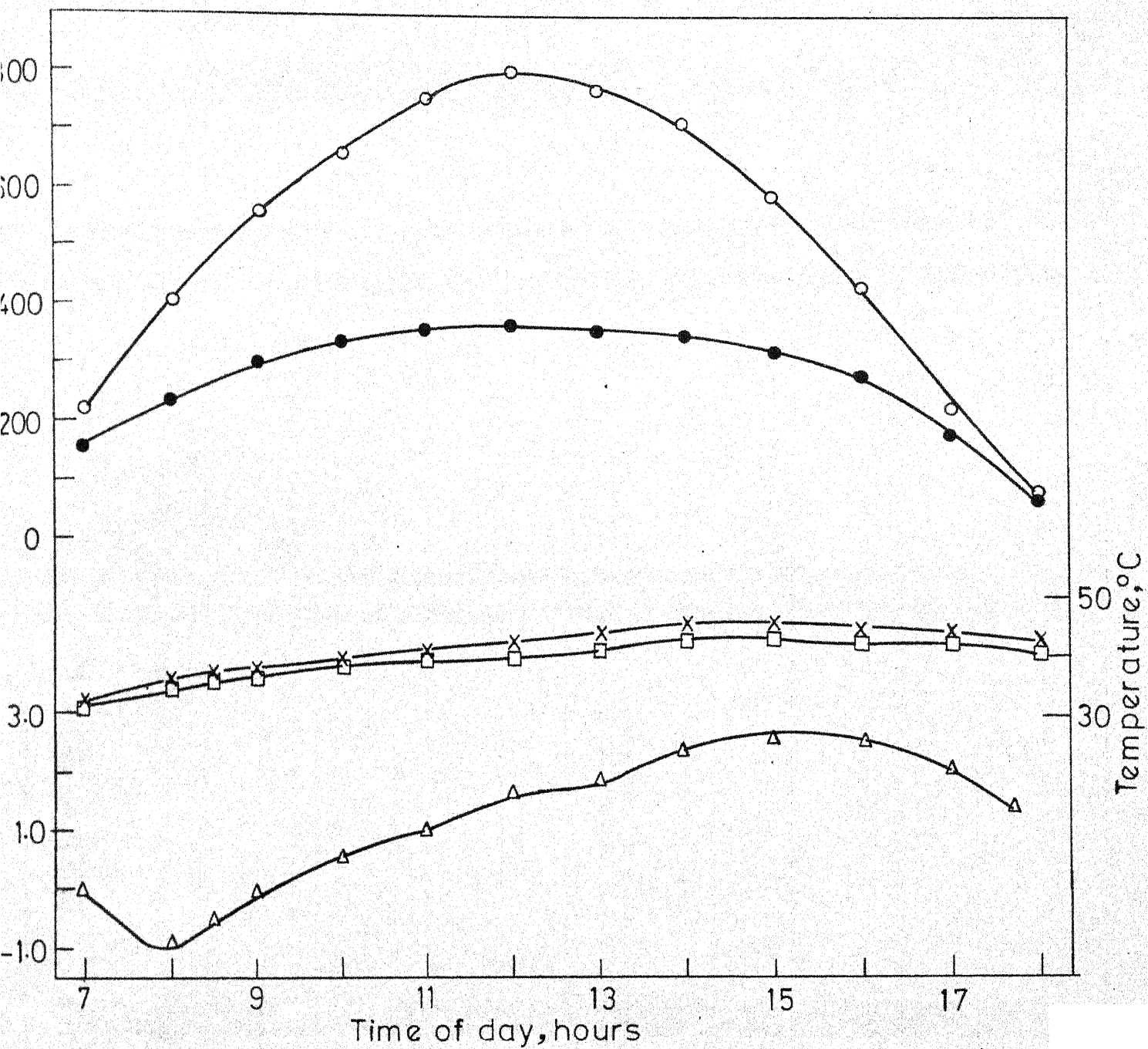
TABLE 4.2 : Experimental Data and Results for test in Continuous Flow

Date	Time		Tilt angle	Mass flow rate (l-g/h)	Energy utilized by flow- ing water (kcal)	Thermal energy gained by system (kcal)	Insolation (kcal)		Total Insolation (kcal)	Total Energy utilized by water (kcal)	Efficiency %	
	From A.M.	To P.M.					Direct	Diffuse				
29.5.74	7.00	6.10	6°	30	1071.0	157.15	1115	539.0	178.0	1832	1228.0	67.0
31.5.74	7.00	6.00	6°	90	1282.5	134.7	1130	686.5	193.5	2010	1417.2	70.3
2.6.74	7.00	5.00	6°	150	1380.0	157.15	1055	759.0	196.0	2010	1537.15	76.4
12.6.74	5.00	5.40	6°	210	961.8	0.0	965	441.0	151.0	1557	961.8	62.0



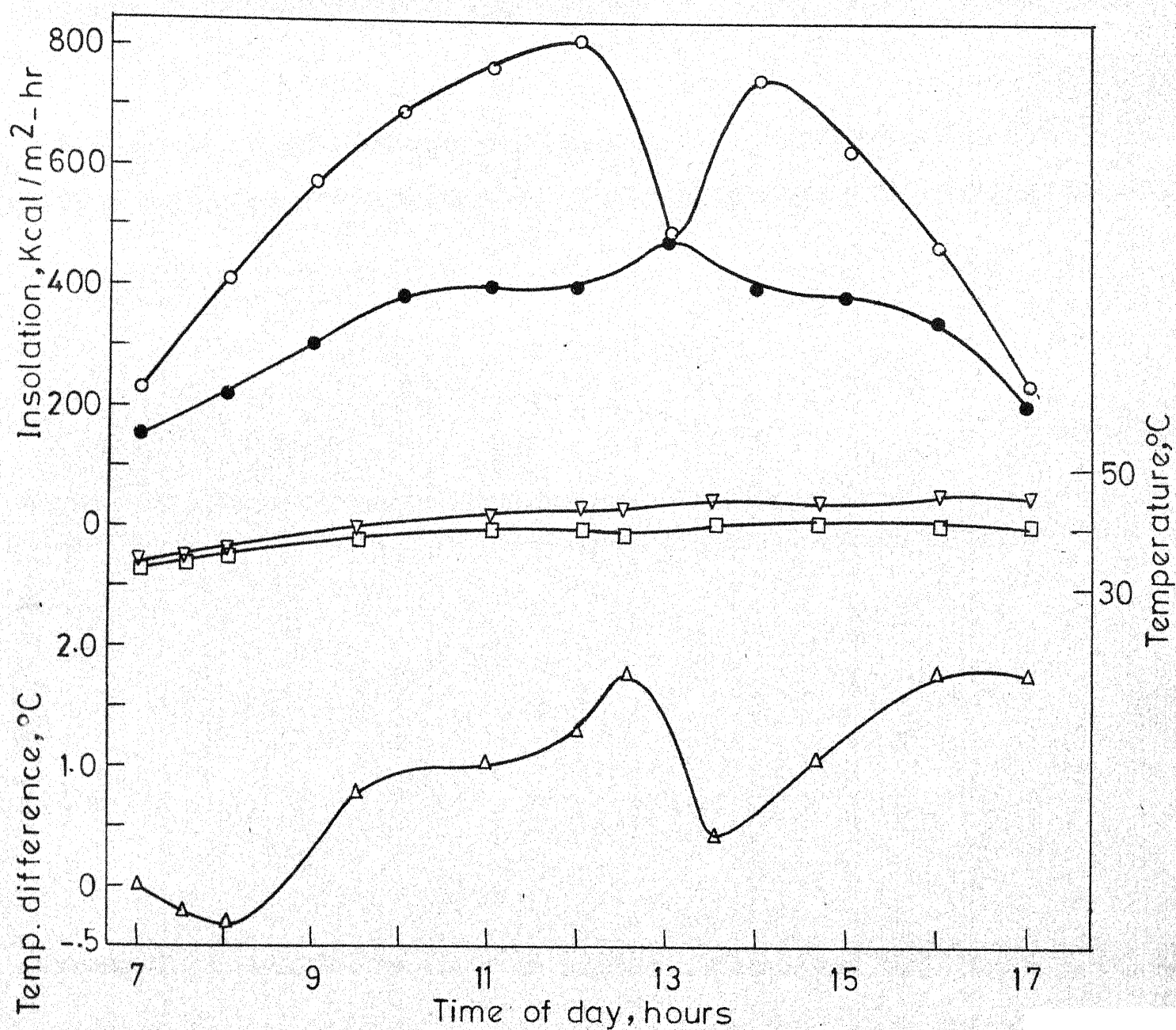
- Direct insolation on the surface of collector $\psi = 6^\circ$
- Diffuse insolation " " " " $\psi = 6^\circ$
- x Outer glass temperature
- Ambient temperature
- △ Difference between water temperature at outlet & inlet

FIG.4.2 Experimental results for test at Kanpur, 29 May, 1974 for mass flow rate of 0.5 Kg/min.



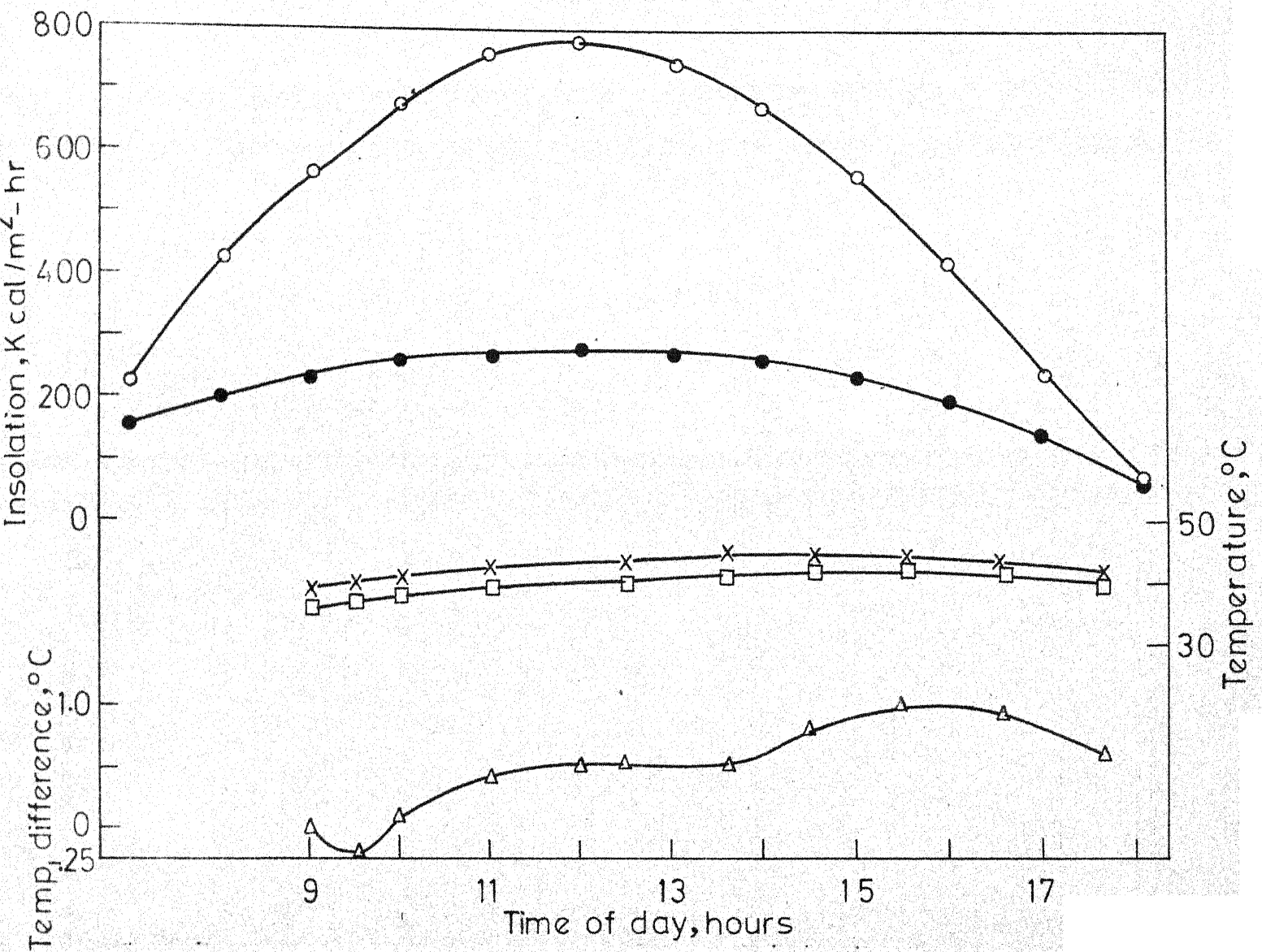
- x Outer glass temperature
- o Direct normal radiation on collector surface $\psi = 6^\circ$
- Diffuse sky radiation " " " " $\psi = 6^\circ$
- Ambient temperature
- △ Difference between water temperature at outlet & inlet

FIG. 4.3 Experimental results for test at Kanpur, 31 May, 1974 for mass flow rate of 1.5 kg/min.



- Direct radiation on collector
- Diffuse sky " " "
- ▽ Outer glass temperature
- Ambient temperature
- Δ Difference between water temp. at outlet & inlet.

FIG.4.4 Experimental results for test at Kanpur, June 2, 1974 for mass flow rate of 2.5 kg/min.



- Direct normal radiation on the collector surface
- Sky diffuse radiation on the collector surface
- x Outer glass temperature
- Ambient temperature
- △ Difference between water temperature at outlet & inlet

FIG. 4.5 Experimental results for test at Kanpur, June 12, 1974 for mass flow rate of 3.5 kg./min.

In all these figures it is seen that the difference between the outlet and the inlet temperatures of water at the initial stage of the experiment is negative and that the time in which this difference remains negative decreases as the mass flow rate increases. A possible explanation for this can be given as follows. In the morning the heater is filled with water at a particular temperature. The inlet water is fed in from a tap which is connected by a long system of G.I. pipes to an overhead tank. Thus the inlet water is warmer than that in the heater pipe. In the early stages of the experiment, this hot incoming water gets mixed with the colder water inside the heater and this becomes cooler. Also in the morning the amount of sun's radiation is not enough to provide as much energy as it has lost in the insulated portion. For the lowest mass flow rate of 0.5 kg/min. the time during which the outlet and inlet water temperature difference remains negative is about 3 hour. As the mass flow rate increases the difference between temperatures of the incoming water and that in insulated section goes on decreasing. Also the time of contact of the incoming water with that in the insulated section reduces. Therefore the time during which the difference between the outlet and inlet water temperature remains negative, decreases. For mass flow rate of 3.5 kg/min. this time reduces to less than an hour.

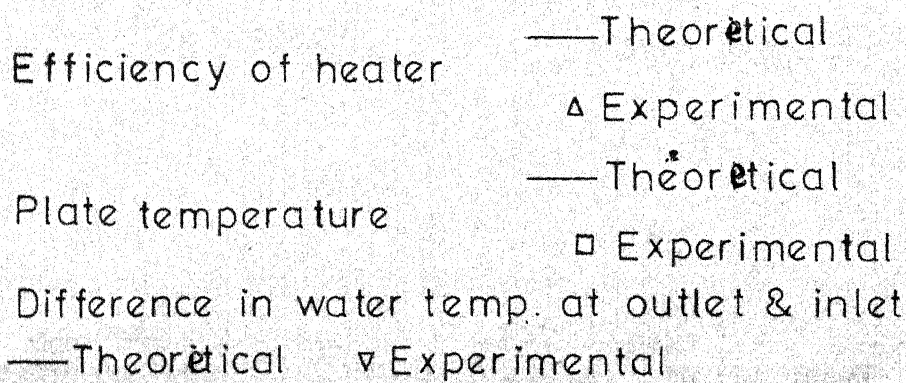
From Table 4.2 it is also seen that the heater efficiency increases with the increase in mass flow rate. As the

mass flow rate is increased the heat transfer coefficient also increases and thus there is better transfer of heat from the tube to the fluid. Also at higher mass flow rates the temperatures of the plate are lower than those at lower mass flow rates and thus there are smaller losses from the plate to outside. A combination of these two effects leads to the observed rise in efficiency. If a second order regression curve is drawn through the data points of efficiency vs. mass flow rate then all the points lie within $\pm 5\%$ of this curve. At lower mass flow rates of 0.5 and 1.5 kg/min the trend shows an increase in efficiency with increase in mass flow rates because of reasons stated above. For higher mass flow rates the trend is difficult to predict since besides the scattering of points due to experimental error there is the problem of flow being not fully developed because of insufficient entry length.

Figure 4.4 shows the experimental data for a mass flow rate of 150 kg/h. There is a sudden dip in the incident radiation of the sun at about 1 p.m. This was because of clouds. This effects the water temperature difference which also dips at 1.30 p.m.

Finally the experimental results are compared with those obtained theoretically. Figure 4.6 shows the comparison for efficiency, plate temperature and difference between water temperature at the outlet and inlet, for varying mass flow rates of 0.5 kg/min. to 3.5 kg/min.

Table 4.3 lists the various quantities, both experimental and theoretical. The theory compares reasonably well with the experimental results obtained. The difference between the theoretical and experimental results for mass flow rates of 30 kg/h to



1994, 1995, 1996, 1997, 1998, 1999, 2000, 2001, 2002, 2003, 2004, 2005, 2006, 2007, 2008, 2009, 2010, 2011, 2012, 2013, 2014, 2015, 2016, 2017, 2018, 2019, 2020, 2021, 2022, 2023, 2024, 2025, 2026, 2027, 2028, 2029, 2030, 2031, 2032, 2033, 2034, 2035, 2036, 2037, 2038, 2039, 2040, 2041, 2042, 2043, 2044, 2045, 2046, 2047, 2048, 2049, 2050, 2051, 2052, 2053, 2054, 2055, 2056, 2057, 2058, 2059, 2060, 2061, 2062, 2063, 2064, 2065, 2066, 2067, 2068, 2069, 2070, 2071, 2072, 2073, 2074, 2075, 2076, 2077, 2078, 2079, 2080, 2081, 2082, 2083, 2084, 2085, 2086, 2087, 2088, 2089, 2090, 2091, 2092, 2093, 2094, 2095, 2096, 2097, 2098, 2099, 2100, 2101, 2102, 2103, 2104, 2105, 2106, 2107, 2108, 2109, 2110, 2111, 2112, 2113, 2114, 2115, 2116, 2117, 2118, 2119, 2120, 2121, 2122, 2123, 2124, 2125, 2126, 2127, 2128, 2129, 2130, 2131, 2132, 2133, 2134, 2135, 2136, 2137, 2138, 2139, 2140, 2141, 2142, 2143, 2144, 2145, 2146, 2147, 2148, 2149, 2150, 2151, 2152, 2153, 2154, 2155, 2156, 2157, 2158, 2159, 2160, 2161, 2162, 2163, 2164, 2165, 2166, 2167, 2168, 2169, 2170, 2171, 2172, 2173, 2174, 2175, 2176, 2177, 2178, 2179, 2180, 2181, 2182, 2183, 2184, 2185, 2186, 2187, 2188, 2189, 2190, 2191, 2192, 2193, 2194, 2195, 2196, 2197, 2198, 2199, 2200, 2201, 2202, 2203, 2204, 2205, 2206, 2207, 2208, 2209, 2210, 2211, 2212, 2213, 2214, 2215, 2216, 2217, 2218, 2219, 2220, 2221, 2222, 2223, 2224, 2225, 2226, 2227, 2228, 2229, 2230, 2231, 2232, 2233, 2234, 2235, 2236, 2237, 2238, 2239, 2240, 2241, 2242, 2243, 2244, 2245, 2246, 2247, 2248, 2249, 2250, 2251, 2252, 2253, 2254, 2255, 2256, 2257, 2258, 2259, 2260, 2261, 2262, 2263, 2264, 2265, 2266, 2267, 2268, 2269, 2270, 2271, 2272, 2273, 2274, 2275, 2276, 2277, 2278, 2279, 2280, 2281, 2282, 2283, 2284, 2285, 2286, 2287, 2288, 2289, 2290, 2291, 2292, 2293, 2294, 2295, 2296, 2297, 2298, 2299, 2300, 2301, 2302, 2303, 2304, 2305, 2306, 2307, 2308, 2309, 2310, 2311, 2312, 2313, 2314, 2315, 2316, 2317, 2318, 2319, 2320, 2321, 2322, 2323, 2324, 2325, 2326, 2327, 2328, 2329, 2330, 2331, 2332, 2333, 2334, 2335, 2336, 2337, 2338, 2339, 2340, 2341, 2342, 2343, 2344, 2345, 2346, 2347, 2348, 2349, 2350, 2351, 2352, 2353, 2354, 2355, 2356, 2357, 2358, 2359, 2360, 2361, 2362, 2363, 2364, 2365, 2366, 2367, 2368, 2369, 2370, 2371, 2372, 2373, 2374, 2375, 2376, 2377, 2378, 2379, 2380, 2381, 2382, 2383, 2384, 2385, 2386, 2387, 2388, 2389, 2390, 2391, 2392, 2393, 2394, 2395, 2396, 2397, 2398, 2399, 2400, 2401, 2402, 2403, 2404, 2405, 2406, 2407, 2408, 2409, 2410, 2411, 2412, 2413, 2414, 2415, 2416, 2417, 2418, 2419, 2420, 2421, 2422, 2423, 2424, 2425, 2426, 2427, 2428, 2429, 2430, 2431, 2432, 2433, 2434, 2435, 2436, 2437, 2438, 2439, 2440, 2441, 2442, 2443, 2444, 2445, 2446, 2447, 2448, 2449, 2450, 2451, 2452, 2453, 2454, 2455, 2456, 2457, 2458, 2459, 2460, 2461, 2462, 2463, 2464, 2465, 2466, 2467, 2468, 2469, 2470, 2471, 2472, 2473, 2474, 2475, 2476, 2477, 2478, 2479, 2480, 2481, 2482, 2483, 2484, 2485, 2486, 2487, 2488, 2489, 2490, 2491, 2492, 2493, 2494, 2495, 2496, 2497, 2498, 2499, 2500, 2501, 2502, 2503, 2504, 2505, 2506, 2507, 2508, 2509, 2510, 2511, 2512, 2513, 2514, 2515, 2516, 2517, 2518, 2519, 2520, 2521, 2522, 2523, 2524, 2525, 2526, 2527, 2528, 2529, 2530, 2531, 2532, 2533, 2534, 2535, 2536, 2537, 2538, 2539, 2540, 2541, 2542, 2543, 2544, 2545, 2546, 2547, 2548, 2549, 2550, 2551, 2552, 2553, 2554, 2555, 2556, 2557, 2558, 2559, 2560, 2561, 2562, 2563, 2564, 2565, 2566, 2567, 2568, 2569, 2570, 2571, 2572, 2573, 2574, 2575, 2576, 2577, 2578, 2579, 2580, 2581, 2582, 2583, 2584, 2585, 2586, 2587, 2588, 2589, 2590, 2591, 2592, 2593, 2594, 2595, 2596, 2597, 2598, 2599, 2600, 2601, 2602, 2603, 2604, 2605, 2606, 2607, 2608, 2609, 2610, 2611, 2612, 2613, 2614, 2615, 2616, 2617, 2618, 2619, 2620, 2621, 2622, 2623, 2624, 2625, 2626, 2627, 2628, 2629, 2630, 2631, 2632, 2633, 2634, 2635, 2636, 2637, 2638, 2639, 2640, 2641, 2642, 2643, 2644, 2645, 2646, 2647, 2648, 2649, 2650, 2651, 2652, 2653, 2654, 2655, 2656, 2657, 2658, 2659, 2660, 2661, 2662, 2663, 2664, 2665, 2666, 2667, 2668, 2669, 2670, 2671, 2672, 2673, 2674, 2675, 26

150 kg/h lies within 11%. The theoretical efficiency is higher since we have assumed in the analysis that the absorber plate is coated with a selectively absorbing paint which has absorptivity of unity and very low emissivity. In the actual test the emissivity of the lamp black coating is also nearly equal to unity. Hence one may expect higher losses due to radiation and a reduced efficiency. Also we have assumed in theoretical calculations that the tube temperature is uniform at any given section whereas this cannot possibly occur in practise owing to non-uniform irradiation over the tube periphery, and the relatively small thermal conductivity of the tube.

Table 4.3 : Comparison of Experimental and Theoretical Results of Heater under Forced Convection Mode.

Mass flow rate kg/h	Efficiency %		Plate Temp. °C		Diff. of outlet and inlet water temp. °C/h	
	Theoretical	Exptl	Theoretical	Exptl	Theoretical	Exptl.
30	74.5	67.0	54.0	49.5	4.12	3.4
90	78.4	70.3	46.5	44.7	1.58	1.29
150	78.35	76.4	45.3	44.0	1.05	0.94
210	78.3	62.0	44.5	43.5	0.64	0.51

It is worthwhile to comment here on the efficiencies reported by Vincze [12]. He has reported efficiencies as high as 216%. There are two probable reasons for such absurdly high efficiencies. One is that Vincze has assumed the radiation falling

The theory compares reasonably well with the experimental results. The smallest difference of 2.8% is found for mass flow rate of 210 kg/h whereas for mass flow rates of 30 and 90 kg/h the differences lie in the range of 10 - 11%. Still from purely heat transfer point of view there is ample scope of improving the theory, and it may be taken up as the next stage of investigation. The variation of solar radiation with time, together with the circumferential temperature variation may be incorporated in the refined theory.

The present study is also a first step towards making an efficient solar collector device which can be used as a generator of a vapor absorption refrigeration system. The temperatures obtained in the present study are not high and in order to obtain higher temperatures a parabolic concentrator can be put below the cylindrical heater. The cylindrical heater has one more advantage over the flat - plate collectors, if used for purposes of generator, and that is that the cylinder can withstand higher pressures easily while in flat plate collectors, bulging of the absorber plate and consequent leakage may set in, if high pressures are used.

REFERENCES

1. A. TOFFLER, Future Shock, Bantam-Books Inc., New York, 1970, p. 23.
2. H. LUSTIG, Our Dwindling Energy Resources, UNESCO Courier, January 1974, pp. 11-12.
3. F.A. BROOKS and W. MILLER, Availability of Solar Energy, Introduction to the Utilization of Solar Energy (Ed. A.M. ZAREM, and D.D. ERWAY), McGraw-Hill, 1963, pp. 30-31.
4. P.E. GLASER, Power From the Sun, UNESCO Courier, January 1974, pp 16-17.
5. ANONYMOUS, Down on the Solar Farm, UNESCO Courier, January 1974, p. 21.
6. J.I. YELLOT and S. RAINER, An Investigation of Solar Water Heater Performance, Trans. ASHRA-E, Vol. 70, 1964, pp. 425-433.
7. A.G.H. DIETZ, Diathermanous Materials and Properties of Surfaces, Introduction to the Utilization of Solar Energy (Ed. A.M. ZAREM and D.D. ERWAY), McGraw Hill, 1963, p. 85.
8. S.K. RAO and R.K. SURI, Optimization of Flat-Plate Solar Collector Area, Solar Energy, Vol. 12, No. 2, 1969, pp. 531 - 535.
9. J.C.V. CHINMAPA and K. GNANGLINGAM, Performance at Colombo, Ceylon, of a Pressurized Solar Water Heater of the Combined Collector and Storage Type, Solar Energy, Vol. 15, No. 3, 1973, pp. 195-204.
10. H.P. GARG and A. KRISHNAN, Solar Energy Research at Central Arid Zone Research Institute Jodhpur - A Report, Proceedings of the Fifth Meeting, All India Solar Energy Working Group, Indian Institute of Technology Madras, India 1973.
11. R.S. CHAUHAN, Fabrication and Testing of a Collector-cum-Storage Type of Solar Water Heater, M.Tech. Thesis, I.I.T. Kanpur, 1974.
12. S.A. VINCZE, A High Speed Cylindrical Solar Water Heater, Solar Energy, Vol. 13, No. 3, 1971, p. 345.

13. W.M. KAYS, Convective Heat and Mass Transfer, McGraw-Hill, 1966, pp. 139 - 140, and p. 127.
14. F.B. HILDEBRAND, Advanced Calculus for Applications, Prentice-Hall, 1962, pp. 359 - 360.
15. C.B. MORREY, JR., University Calculus, Addison-Wesley, Inc., 1962, p. 179.
16. ASHRAE, Handbook of Fundamentals, 1972, pp. 393 - 394.
17. H.C. HOTTEL and D.D. ERWAY, Collection of Solar Energy, Introduction to the Utilization of Solar Energy, Mc-Graw-Hill, 1963, p. 96.
18. J.L. THREIKELD, Thermal Environmental Engineering, Prentice-Hall, 1970, p. 321.
19. M. JAKOB, Heat Transfer, Vol. 1, John Wiley and Sons, 1958, pp. 540-541.
20. T.N. SESHADRI, et. al, Climatological and Solar Data for India, CBRI, Roorkee, 1969, p. 54.
21. W.M. KAYS, Convective Heat and Mass Transfer, McGraw-Hill, 1966, pp. 227 - 228.
22. H.C. HOTTEL and A.F. SAROFIM, Radiative Transfer, McGraw-Hill, 1967, p. 54 and p. 159.
23. M.G. SALVODORI and M.L. BARON, Numerical Methods in Engineering, Prentice-Hall, 1963, pp. 46-47.
24. A.K. RAJWANSHI, N. RAVICHANDRAN and V. KADAMBI, Efficiency and Length of Cylindrical Solar Water Heaters, Proceedings of the Fifth Meeting, All India Solar Energy Working Group, Indian Institute of Technology, Madras, India, 1973.
25. I.H. SHAMES, Mechanics of Fluids, McGraw-Hill, 1962, p. 294.

ERRATA

<u>Page</u>	<u>Line</u>	<u>Reads</u>	<u>Should Read</u>
(iii)	13	Finally	Last
1	11	hundred	hundred years
1	13	tempering	tampering
2	4	off	of
3	3	energy than	energy that
4	23	maximum work	lot of work
22	12	are determined	are solved
22	22	early closely	earlier closely
23	19	one step computed	computed one step
39	12	this becomes	thus becomes

APPENDIX I

COMPUTER PROGRAM

C W 31 AUGUST 2

IBFTC MAIN

```

      DIMENSION VM(5),AM(5)
      COMMON X,TS,TGI,TGJ,TSH,TGIHC,AP,AQ,TSAN
      REAL NETA(1200)
      READ,(VM(I),AM(I),I=1,5)
      RS=0.5
31  X=(13.9E-5)/RS
      READ,TS,TGI,TGJ
      AP=0.
      AQ=4.
      DO 20 I=1,5
      AP=AP+(EXP((-VM(I))*X)-1.)/(VM(I)*AM(I))
20  AQ=AQ+1./(VM(I)*AM(I))
      TE=TS
      TM=TS
      CALL ALGEQ(TS,TGI,TGJ)
      TSN=TS
      TGIN=TGI
      TGJN=TGJ
      TSI=TS+G(X,TS,TGI)*(AP+AQ)
      CALL ALGEQ(TSI,TGI,TGJ)
      TSH=0.5*(TSI-TSN)+TSN
      TGIH=0.5*(TGI-TGIN)+TGIN
      TGJH=0.5*(TGJ-TGJN)+TGJN
      TGIHO=TGIH
      TSHO=TSH
      TGJHO=TGJH
      CALL DIFEQ
11  TSH=0.5*(TSAN-TSN)+TSN
      CALL ALGEQ(TSH,TGI,TGJ)
      TGIHO=TGI
      TGJHO=TGJ
      TSHO=TSH
      I=1
      KM=1
10  CALL ALGEQ(TSH,TGI,TGJ)
      TGIH=TGI
      TGJH=TGJ
      GO TO 13
12  TGI=TGIHO
      TGJ=TGJHO
      TS=TSHO
      CALL ALGEQ(TSAN,TGI,TGJ)
      TGIHO=TGI
      TGJHO=TGJ
      TSHO=TSAN
      CALL DIFEQ
      TSH=TSAN
      GO TO 10
13  TM=TM+4.*G(X,TSH,TGIH)
      NETA(I)=41.7*RS*(TM-TE)/FLOAT(I)
      IF(I.NE.1) GO TO 14
      AX=0.01*FLOAT(I)
      PRINT17,AX,NETA(I),TSH,TGIH,TGJH,TM
17  FORMAT(F10.2,F12.4,F12.2)
      GO TO 21
14  IF((I-KM).NE.39) GO TO 21
```

```

      AX=0.01*FLOAT(I)
      PRINT18,AX,NETA(I),TSH,TGIH,TGJH,IM
18  FORMAT(F10.2,F12.4,4F12.2)
      KM=I+1
21  I=I+1
      IF(I.GE.1000) GO TO 16
      GO TO 12
16  IF(RS.GE.6.5) GO TO 22
      RS=RS+1.
      GO TO 31
22  STOP
      END
£IBFTC G
      FUNCTION G(X,A,B)
      G=0.298*X*(113.-0.48*(A-B)-(15.1E-10)*((273.16+A)**4-(273.16+B)
14))
      RETURN
      END
£IBFTC ALGEQ
      SUBROUTINE ALGEQ(TS,TGI,TGJ)
      DATA A,B,C,D,R,F,Q,H,AI/0.928,1.85E-8,11.35,8.40,2.74E-8,96.1E8,
18.40,0.48,1.51E-9/
25  SAI=(273.16+TGI)**4
      SAJ=(273.16+TGI)**3
      SBJ=(273.16+TGJ)**3
      SBI=(273.16+TGJ)**4
      SS=(273.16+TS)**4
      FU=A*(TGI-TGJ)+B*(SAI-SBI)+C-D*(TGJ-39.9)-R*0.94*(SBI-F)
      GU=A*(TGI-TGJ)+B*(SAI-SBI)-Q-H*(TS-TGI)-AI*(SS-SAI)
      DIFFUI=A+4.*B*SAJ
      DIFFUJ=-A-4.*B*SBJ-D-4.*R*.94*SBJ
      DIFGUI=A+4.*B*SAJ+H+4.*AI*SAJ
      DIFGUJ=-A-4.*B*SBJ
      DENM=DIFFUI*DIFGUJ-DIFGUI*DIFFUJ
      Y=-(FU*DIFGUJ-GU*DIFFUJ)/DENM
      Z=(FU*DIFGUI-GU*DIFFUI)/DENM
      TGI=TGI+Y
      TGJ=TGJ+Z
      IF(ABS(FU).GE.0.001) GO TO 25
      IF(ABS(GU).GE.0.001) GO TO 25
      RETURN
      END
£IBFTC DIFEQ
      SUBROUTINE DIFEQ
      COMMON X,TS,TGI,TGJ,TSHO,TGIHO,AP,AQ,TSAN
      U=G(X,TSHO,TGIHO)
      TSAN=TS+U*(AP+AQ)
10  CALL ALGEQ(TSAN,TGI,TGJ)
      TSM=TSAN
      TGIM=TGI
      TSAN=TS+(AP*U+AQ*G(X,TSM,TGIM))
      IF(ABS(TSAN-TSM).GE.0.005) GO TO 10
      RETURN
      END
£ENTRY
25.68,-.007630,83.86,-.002058,174.2,-.000901,296.5,-.000487,450.9,-.000297
42.,41.,38.
42.,41.,38.

```